PaleoBios 36: 1–18, July 15, 2019

PaleoBios

OFFICIAL PUBLICATION OF THE UNIVERSITY OF CALIFORNIA MUSEUM OF PALEONTOLOGY

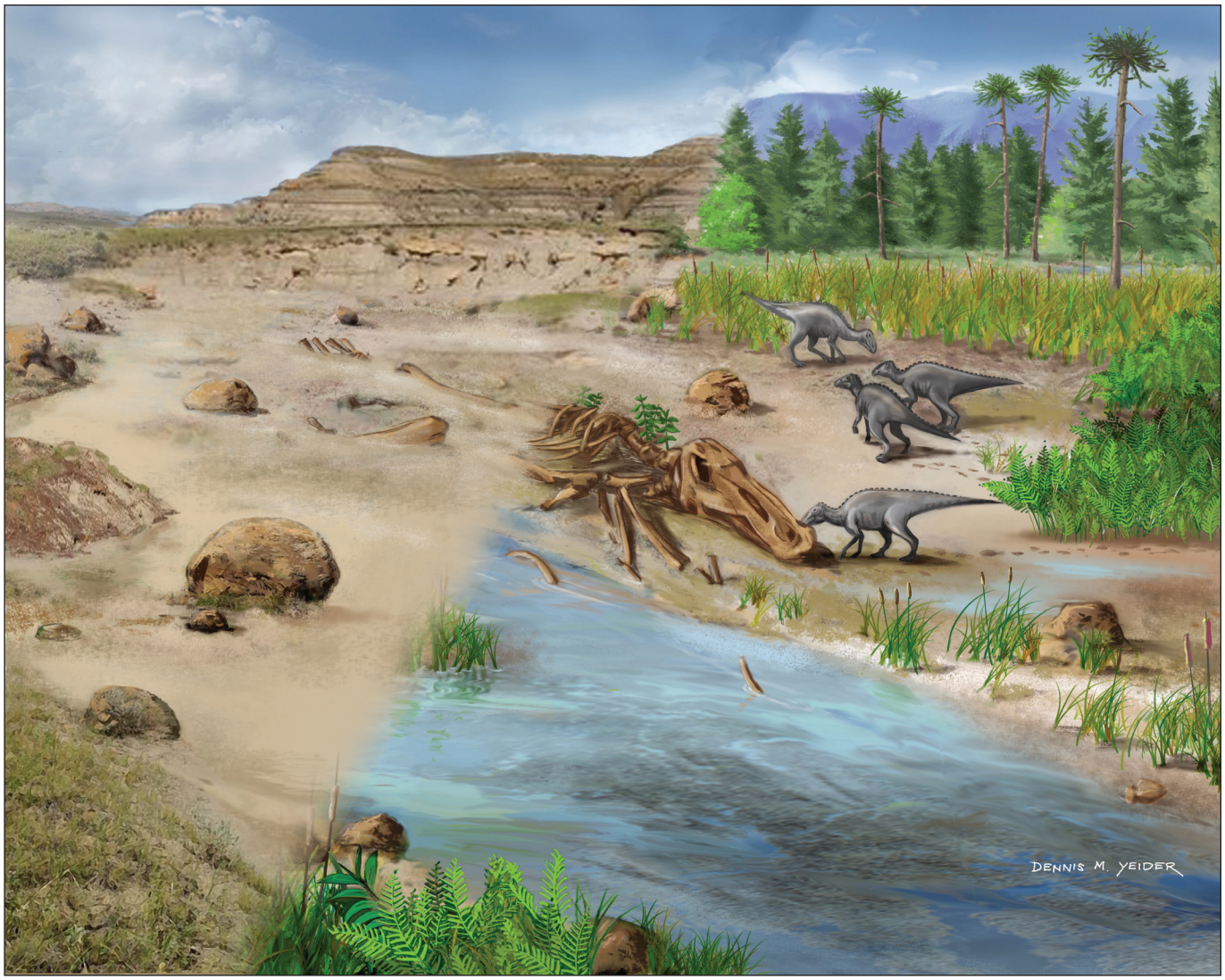

MATEUSZ WOSIK, MARK B. GOODWIN & DAVID C. EVANS (2019). Nestling-sized hadrosaurine cranial material from the Hell Creek Formation of northeastern Montana, USA, with an analysis of cranial ontogeny in *Edmontosaurus annectens*.

Cover: *Edmontosaurus* nestlings, similar to many other duck-billed dinosaurs, segregated from adults likely forming their own independent groups. Here, one of these groups encounters the skeletal remains of an adult, which demonstrates the size difference between nestlings and adults. This reconstruction of the Sandstone Basin locality is split into a present field photograph (left) and past interpretation (right) to demonstrate the significant environmental changes over 66 million years. Artwork by D. M. Yeider.

Citation: Wosik, M., M.B. Goodwin, and D.C. Evans. 2019. Nestling-sized hadrosaurine cranial material from the Hell Creek Formation of northeastern Montana, USA, with an analysis of cranial ontogeny in *Edmontosaurus annectens*. *PaleoBios*, 36. ucmp_paleobios_44525.

Nestling-sized hadrosaurine cranial material from the Hell Creek Formation of northeastern Montana, USA, with an analysis of cranial ontogeny in *Edmontosaurus annectens*

MATEUSZ WOSIK[1,2*], MARK B. GOODWIN[3] and DAVID C. EVANS[2,4]

[1]Misericordia University, 301 Lake Street, Dallas, PA, USA, *mwosik@misericordia.edu;*
[2]Department of Ecology and Evolutionary Biology, University of Toronto, 100 Queen's Park, Toronto, Ontario, M5S 2C6, Canada;
[3]Museum of Paleontology, University of California, 1101 Valley Life Sciences Bldg., Berkeley, California, 94720, USA, *mark@berkeley.edu*;
[4]Department of Natural History, Royal Ontario Museum, 100 Queen's Park, Toronto, Ontario, M5S 2C6, Canada, *d.evans@utoronto.ca*

Despite over a century of intense collecting, the Hell Creek Formation has produced exceedingly few specimens of small juveniles and nestling-sized dinosaurs. Here, we report on the first cranial material of nestling-sized hadrosaurid dinosaurs from the formation. The specimens were recovered from the Sandstone Basin locality in Garfield County, northeastern Montana. The material consists of two dentaries, a surangular, and a quadrate from disassociated individuals, which through ontogenetically independent characters allows assignment of the surangular (UCMP 235857) and quadrate (UCMP 235859) to Hadrosaurinae and the dentary (UCMP 235860) to *Edmontosaurus*. Since *Edmontosaurus annectens* is the only known hadrosaurid in the formation, we hypothesize that these specimens represent the earliest ontogenetic growth stage of *E. annectens* providing a significant ontogenetic extension when assessing aspects of cranial ontogeny in this taxon. Using the newly identified nestling cranial material as end members of ontogenetic series for each element in *E. annectens*, we evaluated ontogenetic variability in phylogenetic characters associated with these elements that are used in assessing phylogenetic relationships among hadrosaurids. Although the quadrate and surangular generally develop isometrically and show minimal ontogenetic variation in morphology, the dentary undergoes significant ontogenetic changes. In particular, the dental battery exhibits a high degree of intraspecific variability through ontogeny. Ontogenetic variability in the dentary should reflect a commensurate degree of variation in the jaws and facial skeleton, suggesting caution should be used when taxonomically identifying small edmontosaur material, such as that known from Alaska. Taxonomic identification of new taxa should be restricted to adult individuals until enough specimens are available to adequately assess taxonomic variation in ontogenetically equivalent semaphorants/ontogimorphs for a large range of complementing taxa.

Keywords: *Edmontosaurus*, Hell Creek Formation, Hadrosauridae, dinosaur, ontogeny, nestling

INTRODUCTION

The Late Cretaceous Hell Creek Formation (~ 66–68 mya) of the northwestern United States preserves one of the richest dinosaur fossil assemblages in North America (e.g., Hartman 2002, Pearson et al. 2002, Russell and Manabe 2002, Horner et al. 2011, Lyson and Longrich 2011, Clemens and Hartman 2014, Scannella and Fowler 2014, Fastovsky and Bercovici 2016). To date, specimens representing at least 22 genera of both large and small-bodied dinosaurs have been recognized from this unit (Russell and Manabe 2002) ranging from individual bones (Russell and Manabe 2002) and associated individual skeletons (e.g., Brown 1907, Garstka and Burnham 1997, Horner et al. 2011, Lyson and Longrich

**author for correspondence*

Citation: Wosik, M., M.B. Goodwin, and D.C. Evans. 2019. Nestling-sized hadrosaurine cranial material from the Hell Creek Formation of northeastern Montana, USA, with an analysis of cranial ontogeny in *Edmontosaurus annectens*. *PaleoBios*, 36. ucmp_paleobios_44525.
Permalink: https://escholarship.org/uc/item/6106g279

2011) to monodominant bonebeds (e.g., Christians 1992, Colson et al. 2004, Mathews et al. 2009, Keenan and Scannella 2014, Ullmann et al. 2017). However, the remains of eggs (Jackson and Varricchio 2016), perinates, and juvenile individuals (Tokaryk 1997, Carpenter 1982, Goodwin et al. 2006, Wosik et al. 2017) have been notably scarce. This pronounced rarity has been attributed to historical collection bias favoring larger museum-quality specimens (Horner and Goodwin 2006, Goodwin and Horner 2014), together with taphonomic biases against the preservation of small skeletons (e.g., Brown et al. 2013). Only recently was the first documented occurrence of a nestling-sized dinosaur skeleton from the Hell Creek Formation described from a partial post-cranial skeleton referred to *Edmontosaurus annectens* Marsh, 1892 (Wosik et al. 2017). Unfortunately, the skull was not preserved in this exceptional specimen, making it impossible to investigate the cranial anatomy of *E. annectens* nestlings.

Here we describe a collection of the smallest known *E. annectens* cranial material and present a detailed morphological comparison of the dentary, surangular, and quadrate bone elements of *E. annectens* across development stages from nestling to adult. This new information allows more rigorous assessment of characters used in phylogenetic analyses of hadrosaurid dinosaurs (e.g., Prieto-Márquez 2010, Xing et al. 2014, 2017) and the taxonomic validity of the recently erected hadrosaurine *Ugrunaaluk kuukpikensis* Mori et al., 2016, which is exclusively based on juvenile specimens (Mori et al. 2016). We also propose a higher degree of intraspecific variability through ontogeny than previously documented in *Edmontosaurus*, based on this new material and comparison with other hadrosaurids.

LOCALITY

The specimens were surface collected on Bureau of Land Management land from the Sandstone Basin locality (UCMP locality V80092), Garfield County, northeastern Montana (Fig. 1). *In-situ* and weathered bone originates from a series of stacked channels with multiple lag deposits in a complex of cut-and-fill cross-stratified channel sandstones in the upper Hell Creek Formation, about 10–15 meters below the top of the Hell Creek Formation (Sprain et al. 2015).

MATERIALS AND METHODS

The material consists of a nearly complete right dentary (UCMP 235860; Fig. 2A–E), an incomplete and edentulous posterior portion of a right dentary dental battery (UCMP 283755; Fig. 2F–I), an incomplete right surangular (UCMP 235857; Fig. 3), and an incomplete right quadrate (UCMP 235859; Fig. 4). Each element was found disarticulated and dissociated.

The osteology of each specimen is described individually

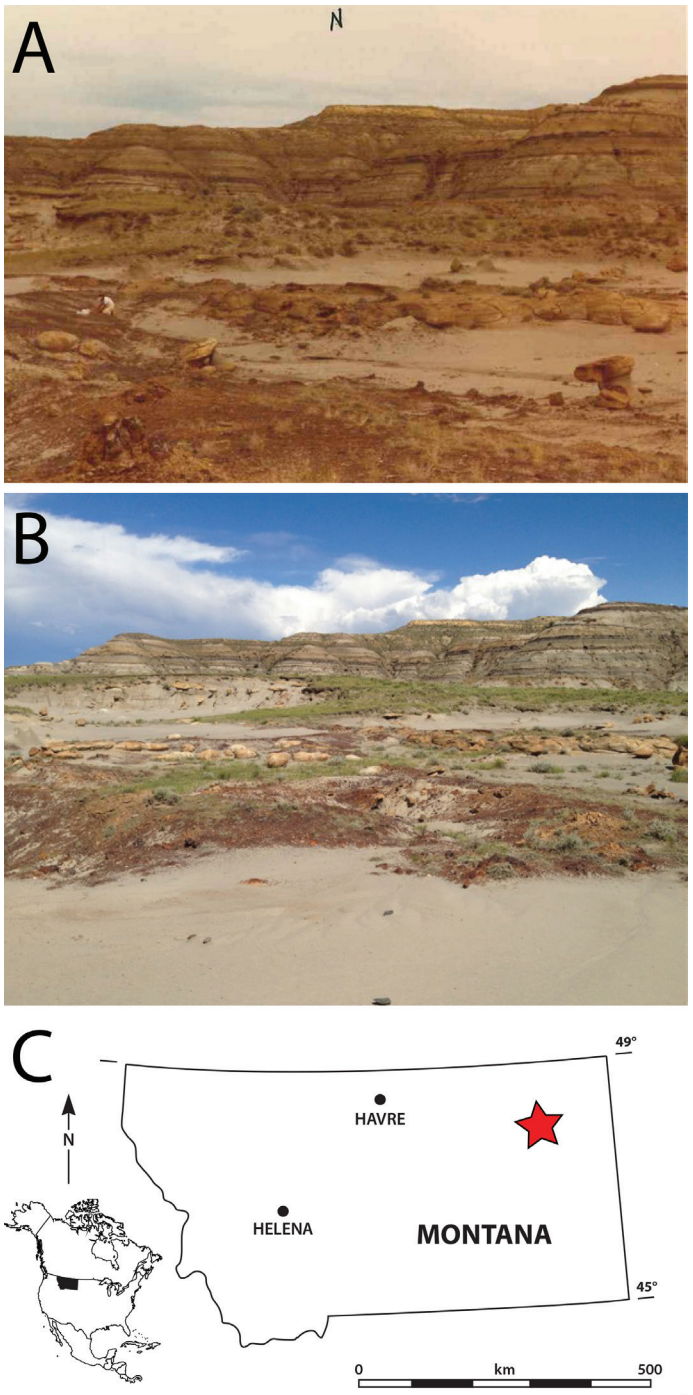

Figure 1. Sandstone Basin UCMP locality V80092 (modified from Wosik et al., 2017). **A**. 1983 field photograph with UCMP paleontologist J.H. Hutchison for scale. **B**. 2016 field photograph demonstrating ~33 years of weathering. **C**. Geographic map of Montana with UCMP locality V80092 represented by a star.

and then ontogenetically assessed with larger specimens of *Edmontosaurus annectens* material housed at the Royal Ontario Museum (Figs. 5, 6). Materials used in the ontogenetic assessment consisted of disassociated juvenile bonebed elements (ROM 53521, 53522, 53529, 53530, 53535, 53536) from Niobrara County, Wyoming, a cast of an associated subadult cranium (ROM 73859) from Harding County, South Dakota, an associated adult surangular and quadrate (ROM 64076) from Harding County, South Dakota, an associated adult quadrate (ROM 64623) from Harding County, South Dakota, and an exceptionally well-preserved and complete adult cranium (ROM 57100) from Perkins County, South Dakota. Horner et al. (2000) defined ontogenetic growth stages in the hadrosaurine hadrosaurid *Maiasaura peeblesorum* Horner and Makela, 1979 based on osteohistological criteria, body size, and egg, nest, and adult associations. This system was extended to skull measurements by Evans (2010) and is applied herein.

Specimen photographs were taken using a Nikon D5300 DSLR camera with a Tamron AF 18–200 mm f/3.5–6.3 XR Di II LD Aspherical (IF) macro zoom lens (Model A14NII). In addition, 3D models were constructed using a NextEngine 3D laser scanner in ScanStudio and uploaded to MorphoSource as supplementary data (MorphoSource, Media Groups M18980–M18983).

Characters used in this analysis directly correspond with Xing et al. (2017) and consisted of the following: dentary characters 1 and 38–58, surangular characters 59–66, and quadrate characters 129–136 (Appendix 1). Character state scores of the nestling-sized materials, and other ontogenetic stages, are listed in Table 1 for each respective element.

Institutional Abbreviations—LACM, Natural History Museum of Los Angeles Country, Los Angeles, California; **ROM**, Royal Ontario Museum, Toronto, Ontario; **UAMES**, University of Alaska Museum, Fairbanks, Alaska; **UCMP**, University of California Museum of Paleontology, Berkeley, California.

SYSTEMATIC PALEONTOLOGY

ORNITHISCHIA Seeley, 1887
ORNITHOPODA Marsh, 1881
IGUANODONTIA Dollo, 1888
HADROSAURIDAE Cope, 1869
HADROSAURINAE Cope, 1869
EDMONTOSAURUS Lambe, 1917
EDMONTOSAURUS cf. *ANNECTENS* Marsh, 1892
Figs. 2–4

Referred Specimens—UCMP 235860, nearly complete right dentary; UCMP 283755, incomplete and edentulous posterior portion of a right dentary dental battery; UCMP 235857, incomplete right surangular; UCMP 235859, incomplete right quadrate.

Formation/Age—Hell Creek Formation, latest Maastrichtian.

Locality—Specimens were surface collected from the Sandstone Basin locality (UCMP locality V80092), Garfield County, northeastern Montana (Fig. 1). Both dentaries (UCMP 235860 and UCMP 283755) were found near location No. 4 and the quadrate (UCMP 235859) near location No. 8 (see Supplemental Material Fig. SM1). Detailed locality information is on file at the UCMP. All permissions were obtained for land access, collecting, and curation of these fossils into the UCMP in 1983 and for an additional visit by UCMP field crews in 2016.

Remarks—The material described here was discovered and collected by J. H. Hutchison (UCMP 235860, 283755, 235859) and L. J. Bryant (UCMP 235857), 14 July 1983. Due to their taphonomic and preservational nature, each specimen is tentatively treated here as belonging to separate individuals. Relative size comparisons are discussed below.

DESCRIPTION

Dentary—Both dentaries, UCMP 235857 (Fig. 2A–E) and UCMP 283755 (Fig. 2F–I), are edentulous and vary in their degree of preservation. UCMP 235857 is generally complete but significantly weathered along all surfaces and edges, missing the distal most extremities of processes. UCMP 283755 is only a small fragment preserving the posterior half of an edentulous dental battery and exhibits a break at the base of the coronoid process which identifies it as part of a right dentary. Because of the extreme fragmentary nature of UCMP 283755, any mention of dentary in this description will correspond with the nearly complete UCMP 235857 unless otherwise specified.

The dentary ramus is most robust along the ventral half of the dentary and where the ramus meets the large dorsal extension of the coronoid process towards the posterior region of the jaw. The anterior part of the dentary ramus, is gently anteroventrally deflected forming the symphyseal process and exhibits an angle of 15° with the horizontal posterior part of the ramus similar to *Saurolophus* Brown, 1912 and *Shantungosaurus* Hu, 1973 (Character 41 [0]). The dentary likely contacted the predentary anterodorsally and anterolaterally and met its counterpart anteromedially at the mandibular symphysis, which is not preserved. The angle between the horizontal axis of the dentary and the slope of the

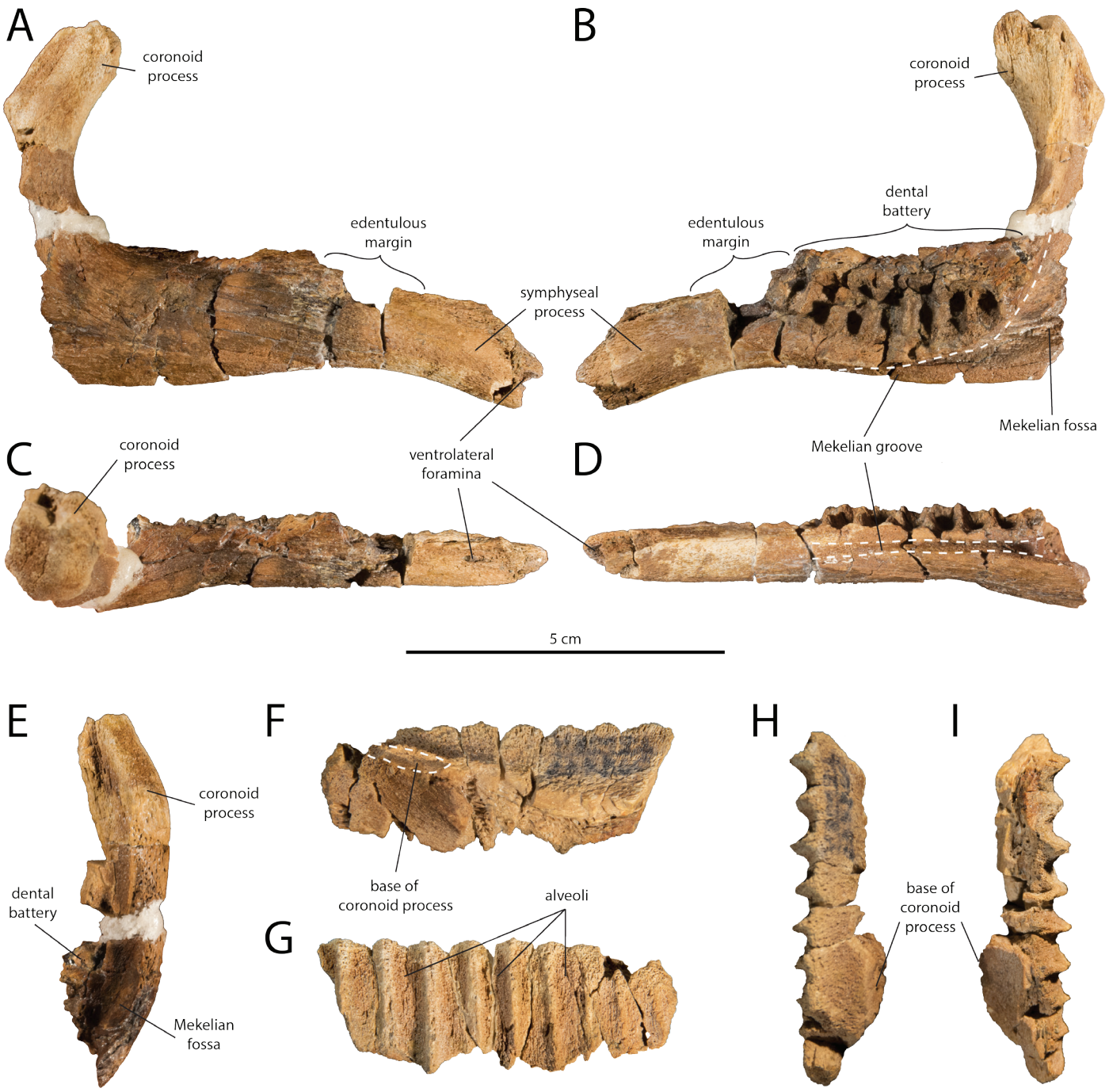

Figure 2. Right dentaries of *Edmontosaurus* cf. *annectens*. UCMP 235860 in lateral (**A**), medial (**B**), dorsal (**C**), ventral (**D**) and posterior (**E**) views. UCMP 283755 in lateral (**F**), medial (**G**), dorsal (**H**) and ventral (**I**) views.

dorsal anterior region that contacts the predentary forms a 132° angle similar only to *Prosaurolophus* Brown, 1916, *Saurolophus*, and *Shantungosaurus* within Hadrosaurinae (Character 40 [0]). Several ventrolaterally facing foramina can be observed in lateral view with the anterior most appearing to be the largest and deepest. Posterior to this along the dorsal margin of the dentary is a long diastema, but poor preservation of this region makes it difficult to precisely describe the orientation of this edentulous margin.

Posterior to the edentulous margin is the dental battery which extends posteriorly to about the midpoint of

the coronoid process. Both dental batteries are edentulous but each preserves a minimum of nine alveoli (Character 1 [0]) where teeth attached via a soft-tissue periodontal ligament (LeBlanc et al. 2016, Bramble et al. 2017). In medial view, the ventral margin of the dental battery is widely arcuate dorsally and distal alveoli are shorter and thinner relative to more central alveoli. Septa of the 2–3 posterior most alveoli in both dentaries are perpendicular to the long axis of the dentary, but anterior alveoli progressively deflect posterodorsally in UCMP 235860 and anterodorsally in UCMP 283755. The dental battery as a whole extends for about half of the anteroposterior length and nearly the entire dorsoventral height of the dentary ramus. In dorsal view, the absence of a lingual curvature of the occlusal surface (Character 55 [1]) delineates UCMP 235860 as a hadrosaurid from hadrosauroids.

The generally complete and robust coronoid process extends the dentary ramus dorsally and slightly laterally before curving anteromedially and is slightly inclined anteriorly to the dorsal margin of the dentary (Character 48 [1]). There is no clear separation between the coronoid process and dental battery (Character 57), but this is likely due to the posteriormost portion of the dental battery being incomplete. The posterior margin of the coronoid process is located posterior to the posterior end of the dental battery, at its current preservation, with minimal overlap (Character 56 [0]). The dorsal terminus of the coronoid process is not well preserved along the margin, but it begins to flatten mediolaterally and expand anteroposteriorly. The surangular would articulate with the posteromedial Meckelian fossa and the splenial and articular with the ventral, anteriorly tapering, Meckelian groove. The water-worn preservation inhibits accurate definition of striations from soft tissue attachment.

Surangular—The surangular, UCMP 235857 (Fig. 3), which is the largest of the three postdentary bones of the lower jaw, only preserves the central body from the proximal base of the retroarticular process to just distal of the anterior termination of the dorsal ridge. Each surface and edge is water worn resulting in a superficially porous texture, which resembles anastomization of vascular canals at the periosteal surface, generally indicative of young individuals (Horner et al. 2000, 2001). The lateral lip is slightly weathered but preserves a rounded D-shaped and symmetrical surface that is dorsoventrally thick. It curves dorsomedially along an obtuse margin and never comes to a sharp apex. In dorsal view, the wide but shallow transverse ridge runs transversely from the apex of the lateral lip to about the center of the dorsal ridge. The

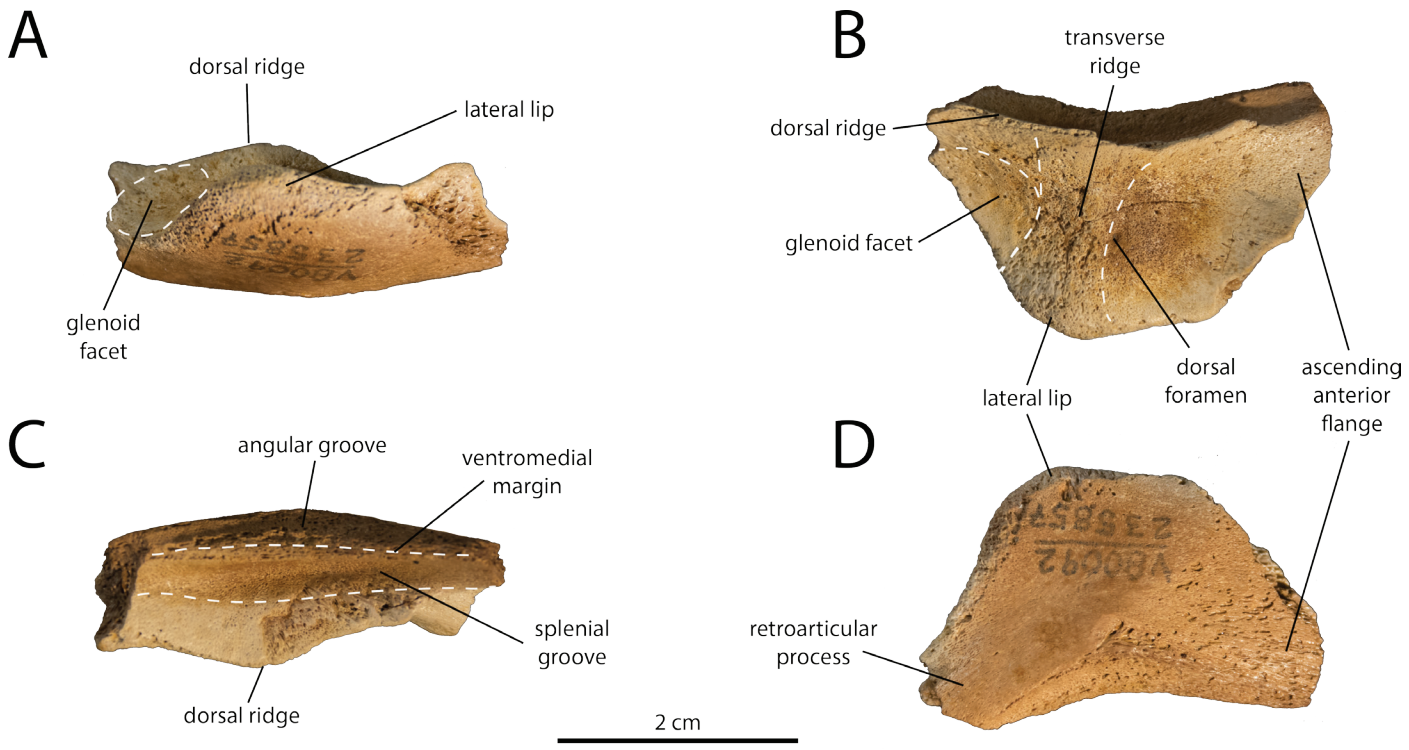

Figure 3. Right surangular of *Edmontosaurus* cf. *annectens*, UCMP 235859 in. lateral (**A**), dorsal (**B**), medial (**C**), and ventral (**D**) views.

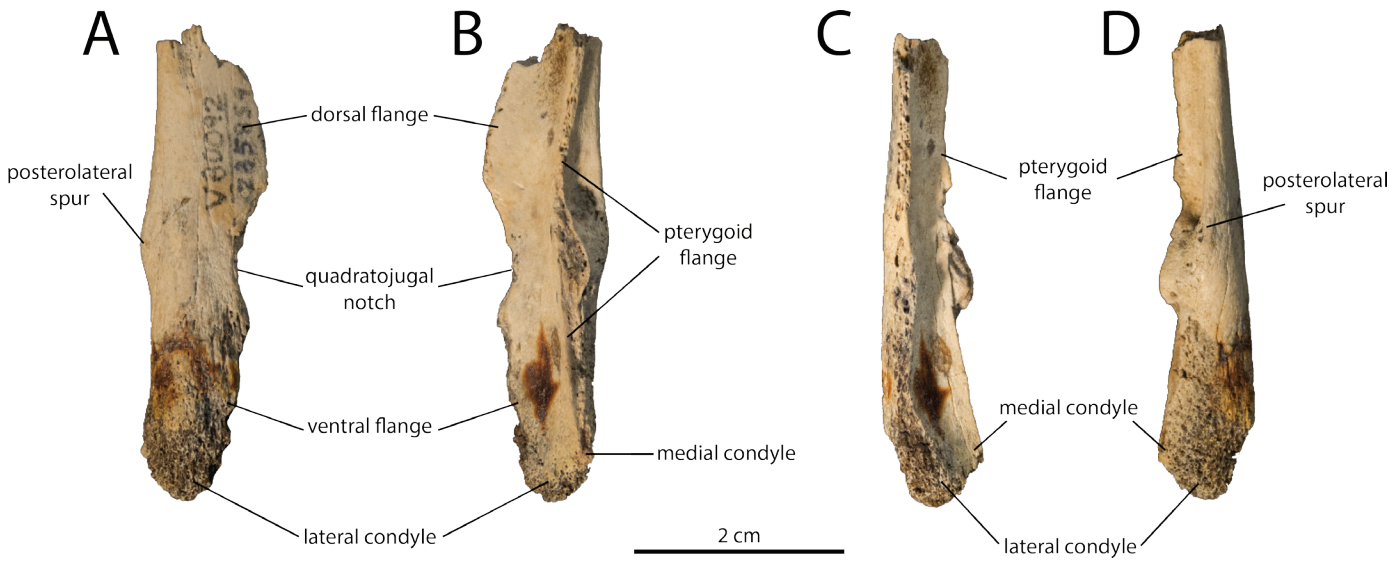

Figure 4. Right quadrate of *Edmontosaurus* cf. *annectens*, UCMP 23585 in lateral (**A**), medial (**B**), anterior (**C**) and posterior (**D**) views.

large, porous concavity posterior to this transverse ridge is the glenoid facet that would articulate with the lateral condyle of the quadrate. A small and shallow dorsal foramen can be observed slightly anterior and central of the transverse ridge. The lack of a lateral foramen (Character 59 [1]) and an accessory foramen (Character 60 [1]) on the anterolateral surface of the surangular positions UCMP 235857 within Hadrosauridae. The dorsal ridge curves ventromedially and widens to become more robust posteriorly. The posterior end is not preserved, but a laterally directed deflection, as part of the posterior expansion, is present. The anterior end gradually meets with the body of the surangular where the ventral rim of the ascending anterior flange continues the path of the dorsal ridge.

The ventromedial margin of the surangular curves parallel with the dorsal ridge at approximately 162° (Character 66 [0]), distinguishing UCMP 235857 from lambeosaurines which have an angle less than 150°. The ventromedial margin separates the articulation surfaces, or grooves, of the splenial and angular, which are dorsal and ventral to the ventromedial margin, respectively. Between the dorsal ridge and the ventromedial margin of the surangular runs the narrow splenial groove, which is deepest at the maximum constriction of the ventromedial margin. Ventral to the ventromedial margin is the angular groove, which is significantly shallower and more porous than the splenial groove. The ventrolateral side of the surangular is convex and exhibits an anteroventral V-shaped region of porous bone that is slightly recessed likely forming a scarf joint with the posterior region of the dentary. The relatively larger ventral expansion of this V-shaped depression and the more ventral orientation of the convex side of the lateroventral surface of the surangular are similar to that observed in *Edmontosaurus*, *Hypacrosaurus* Horner and Currie, 1994, and *Gryposaurus* Lambe, 1914 (Character 62 [2]). Only the proximal base of the ascending anterior flange, which would articulate with the dentary anterolaterally and anteromedially, is preserved along with the base of the robust anterodorsal process.

Quadrate—The quadrate, UCMP 235859 (Fig. 4), is a dorsoventrally elongate bone with a robust vertical ramus that forms the posterolateral margin of the cranium. Two thin, anteriorly directed flanges form the majority of the lateral side of the quadrate and are partitioned by the quadratojugal notch, which is a shallow, symmetrical constriction that is directed anteroposteriorly (Character 132 [1]) and articulated with the quadratojugal and the posterodorsal flange of the jugal. The dorsal flange of the quadrate deflects posterodorsally and thins anteroposteriorly towards the dorsal end, which articulated with the squamosal cotylus. If the dorsal flange were not missing the dorsal half including the quadrate head, the dorsal flange would extend about twice its current length. Because the midpoint of the quadratojugal notch is already located near half the dorsoventral height of the quadrate, the midpoint of the quadratojugal notch would likely be located well below half the dorsoventral height of the quadrate about two thirds distance from

the dorsal quadrate head distinguishing UCMP 235859 from *Maiasaura* and most lambeosaurines (Character 130 [1]). Most of the ventral flange is weathered but a slight anteromedial deflection can be observed.

The lateral condyle, although moderately weathered, is present at the ventral end of the quadrate, which would articulate with the glenoid facet of the surangular, and is significantly larger than the more dorsally elevated and very heavily weathered medial condyle (Character 135 [1]). The posterolateral spur is well preserved and located along the posterior margin of the vertical ramus directly opposite of the minimum constriction of the quadratojugal notch. It forms an arcuate lateral wall for a deep fossa which is bordered medially by the pterygoid flange. The pterygoid flange, which is typically very thin, only preserves the base that runs along the entire medial margin of the quadrate. In medial view, the base of the pterygoid flange has an arcuate shape that deflects posteriorly at both the dorsal and ventral ends. The ventral end of the pterygoid flange meets and terminates at the medial condyle.

ONTOGENETIC ASSESSMENT

Dentary—The robustness of the dentary ramus in *Edmontosaurus annectens* appears to increase proportionately through ontogeny with the length of the dentary (Fig. 5). At the edentulous margin, the ramus significantly begins to thin mediolaterally in juveniles (ROM 53529, 53530) and only the ventral half maintains a robust appearance. The symphyseal process deflects anteroventrally more in juveniles (Character 39 [1]; 152–156°) relative to UCMP 235860 (165°) and subadults (ROM 73859) (162°). The anterior terminus of the symphyseal process strongly curves dorsomedially in subadults to form a flat ventral margin that is parallel with the mandibular symphysis and the horizontal long axis of the dentary (Character 46). This recurving of the mandibular symphysis region begins to occur at the juvenile stage because ROM 53530 exhibits the dorsomedial curving whereas ROM 53529 is still more ventrally oriented and is relatively smaller in size and ontogenetically younger based on linear proportions and alveoli counts, respectively. The ventrolateral foramina vary in size and number through ontogeny without any clear pattern beyond an anteroposterior alignment that follows the thin dorsal half of the dentary ramus and cease around the midpoint of the dental battery.

The length of the diastema is longest in adults (ROM 57100) and makes up a quarter of the total dentary length. The ratio between the length of the edentulous margin anterior to the dentary dental battery and the horizontal distance between the first tooth position and the posterior end of the coronoid process progressively increases with ontogeny (Character 38); UCMP 235860 exhibits a ratio of 0.27 (State 1), juveniles vary from 0.31 (State 1; ROM 53529) to 0.37 (State 2; ROM 53530), and subadults are greater than 0.51 (State 3; ROM 73859). The angle made between the horizontal and the slope of the dentary anterior region that contacts the predentary is slightly larger in adults (Character 40 [0]).

The posterior end of the dental battery extends beyond the posterior margin of the coronoid process in the larger of the two juveniles (ROM 53530) (Character 56). The dental battery increases along the major axes to accommodate the addition and enlargement of tooth rows, also demonstrated histologically by Bramble et al. (2017). The posterodorsal deflection of alveoli is maintained for the anterior region of the dental battery but the larger juvenile dentary also exhibits an anterodorsal deflection of posterior alveoli; the two deflections meet near the coronoid process and alveoli become parallel with the vertical axis of the dentary. Alveoli count also increases through ontogeny from nine in UCMP 235860 to 44 in the subadult (Character 1).

The coronoid process generally becomes more robust and the base expands further laterally. The slight anterior orientation of the coronoid process relative to the horizontal axis observed in UCMP 235860, juveniles, and subadult becomes more anteriorly inclined in adults (Character 48 [2]). The development of the ridge on the medial side of the coronoid process, which is faintly present although not well preserved in UCMP 235860, becomes more developed and posteriorly expanded through ontogeny (Character 52). The Meckelian fossa is deep in juveniles such that the posteroventral region of the dental battery creates a distinct overhang that tapers posteriorly. The Meckelian groove also becomes deeper and contributes to this overhang gradually tapering to form the ventral margin of the dentary directly dorsal of the anterior most alveolus.

Surangular—The periosteal surfaces of juveniles (ROM 53535, 53536) are demarcated with fine striations and maintain a slightly porous exterior, although markedly less than UCMP 235857. The periosteal surface of the adult (ROM 64076) exhibits a high degree of scarring and deep striations, which are occasionally inter-weaving particularly near areas of soft tissue attachment. The lateral lip is asymmetrical in juveniles with a sharper apex that is anteriorly directed. The glenoid facet is also slightly porous in juveniles but begins to develop heavy

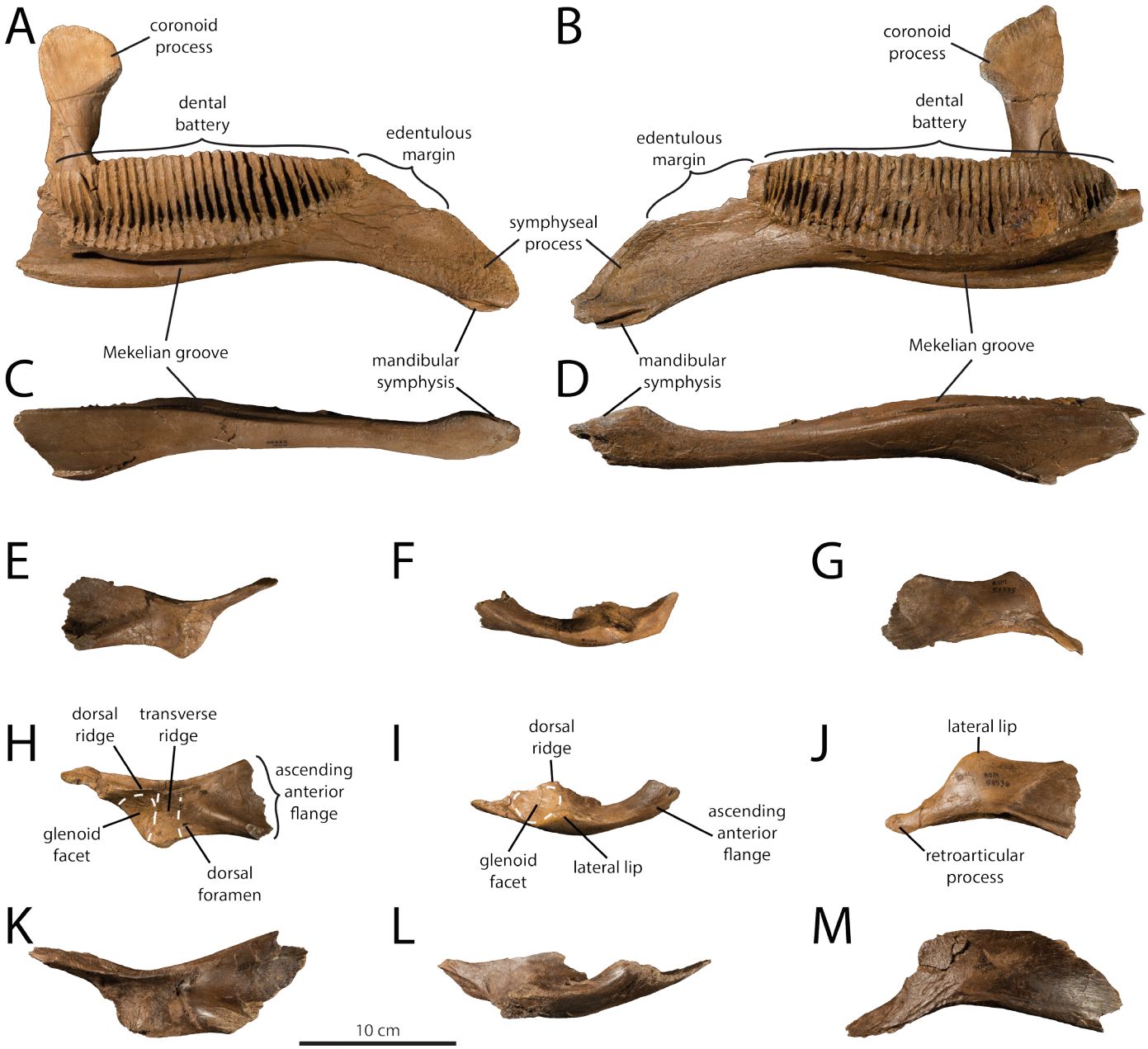

Figure 5. Disarticulated dentaries and surangulars of *Edmontosaurus annectens* used in ontogenetic comparison. **A, C**. Left dentary in medial and ventral view, ROM 53529. **B, D**. Right dentary in medial and ventral view, ROM 53530. **E–G**. Right surangular in dorsal, lateral, and ventral views, ROM 53535. **H–J**. Left surangular in dorsal, lateral, and ventral views, ROM 53536. **K–M**. Left surangular in dorsal, lateral, and ventral views, ROM 64076.

scarring towards the deepest region of this concavity, similar to the adult condition. The dorsal foramen of juveniles and adults appears to have migrated anterolaterally towards the lateral lip from a central location just anterior of the transverse ridge in UCMP 235857. The anterior end of the dorsal ridge terminates sharply and forms a slight overlap in juveniles and adults, which is significantly different from the gradual decline of UCMP 235857. The splenial and articular grooves are much deeper in juveniles and adults and exhibit a narrow, subtriangular shelf that extends medially and slightly dorsally from the middle of the dorsal surface. This subtriangular shelf is best developed in adults and more elongated anteroposteriorly than in juveniles. In ventral view, the anteroventral V-shaped region is progressively more depressed with adults exhibiting the most extreme condition and exhibits strong anteroposteriorly oriented striations with minimal porosity. In dorsal view, the

concavity of the ascending anterior flange in juveniles is significantly more excavated dorsomedially than in UCMP 235857 forming a thin slate of bone for the mandibular adductor fossa. Adults have a similarly deep excavated region but it is bounded with a more gradual transition from the body of the surangular, whereas the rim edges of juveniles are sharper and more pronounced.

Quadrate—In posterior and anterior views, the vertical ramus maintains a straight and vertical orientation through ontogeny (Fig. 6). Juveniles (ROM 53521, 53522) and adults (ROM 57100, 64076, 64623) have a much larger lateral exposure for articulation of the quadratojugal than UCMP 235857, where it is almost nonexistent (Character 136). The quadratojugal notch forms a scarf joint with the quadratojugal along the anterodorsal half of the notch, which is well-developed in juveniles and especially adults but not present in UCMP 235859.

The robustness and posterior deflection of the vertical ramus increases through ontogeny and the pterygoid flange, including its base, becomes proportionately more arcuate. The posteriorly directed deflection of the ventral half is only slightly exhibited in UCMP 235857 and juveniles but is prominent in adults and leads to a wider and more robust lateral condyle. Although the degree of curvature in lateral view cannot be precisely determined in UCMP 2358 because the dorsal half of the dorsal flange is not preserved, the angle between the long axes of the dorsal and ventral flanges of the quadrate range from 145°–162° through ontogeny (Character 129). The lateral condyle, which articulates with the mandibular glenoid of the surangular, expands through ontogeny while the medial condyle appears to undergo a reduction in size relative to the lateral condyle (Character 134). The elevation of the medial condyle relative to the lateral condyle increases through ontogeny where the medial condyle is remarkably elevated in adults but less so in UCMP 235859 and juveniles (Character 135 [1]).

Along the posteroventral margin of the ventral half of the quadrate is a feature that resembles a muscle attachment site; this feature is proportionately largest in UCMP 235859 and reduces through ontogeny until it is completely lost in the adult. The striated markings present in juveniles and adults along the margins of each flange are not present in UCMP 235859. Although the squamosal buttress near the quadrate head is not preserved in UCMP 235859, juveniles and adults have nearly identical morphologies that proportionately increase in size and robustness with the quadrate (Character 133 [0]). The posterolateral spur is rounded and just slightly rises above the surface of the body of the quadrate in UCMP 235857, is well-developed in juveniles with significant detail for soft tissue attachment, and varies in adults between the juvenile condition (ROM 64623) and a more gracile and rounded appearance (ROM 64076). Although

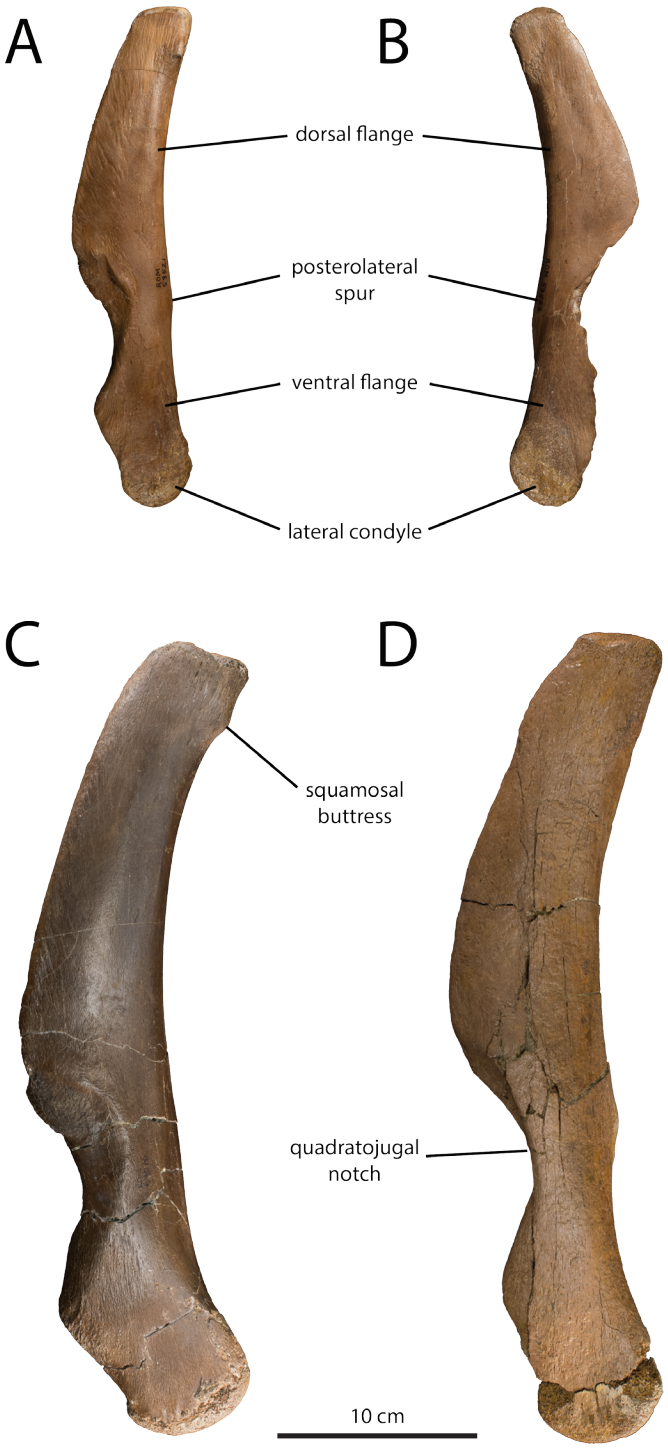

Figure 6. Lateral views of disarticulated quadrates of *Edmontosaurus annectens* used in ontogenetic comparison. **A**. ROM 53521. **B**. ROM 53522. **C**. ROM 64076. **D**. ROM 64623.

the neighboring fossa expands in size through ontogeny, its degree of excavation varies within and between size classes. The ridge extending along the dorsoventral height of the vertical ramus in posterior view exhibits a similar level of variation. Dorsal of the posterolateral spur, the ridge is relatively thinner in some juveniles (ROM 53522) and adults (ROM 64623), and the ventral portion in the same specimens is relatively thicker and less pronounced. This variation does not seem to be related to the degree of excavation of the fossae that neighbor the posterolateral spur.

DISCUSSION

This collection represents the smallest known cranial elements of a hadrosaurine from the penecontemporaneous Late Cretaceous Hell Creek, Lance, and Frenchman formations. A combination of ontogenetically invariable morphological characters supports our assignment of the surangular (UCMP 235857) and quadrate (UCMP 235859) to Hadrosaurinae and the dentary (UCMP 235860) to *Edmontosaurus*. Although none of the autopomorphies of *E. annectens* are present, we tentatively refer these specimens to this taxon because it is the only *Edmontosaurus* species known from the Hell Creek Formation despite over a century of rigorous collecting and prospecting (Campione and Evans 2011, Horner et al. 2011, Prieto-Márquez 2014).

The nearly complete dentary (UCMP 235860) has a total length of 78 mm and is comparable in size to hadrosaurid nestlings from Dinosaur Provincial Park (e.g., TMP 1996.012.0012 [65 mm]; Tanke and Brett-Surman 2001), the Upper Cretaceous of New Mexico (KUVP 96980 [70 mm]; Hall 1993), and those of *Hypacrosaurus stebingeri* (MOR 548 [77 mm]; Horner and Currie 1994) and *Maiasaura peeblesorum* (YPM 22400 [67 mm]; Prieto-Márquez and Guenther 2018) from the Two Medicine Formation of Montana. Each of these dentaries contain between 9–12 alveoli, where teeth would attach to the jaw via a periodontal ligament (LeBlanc et al. 2016, Bramble et al. 2017) and have a dental battery that accounts for at least half of the total dentary length. Therefore, we assign UCMP 235860 to the late nestling stage of Horner et al. (2000) and Wosik et al. (2017). Although the quadrate (UCMP 235859) does not preserve much of the dorsal half, it is smaller than what would be expected if it were associated with the dentary (UCMP 235860) based on MOR 548 (Horner and Currie 1994), which shares a similar total dentary length to UCMP 235860, but could also be a further example of variation between taxa. Conversely, the surangular (UCMP 235857) has a minimum width of 20 mm between the ventromedial margin and the apex of the lateral lip, which is considerably larger than the corresponding measurement of 12.5 mm in MOR 548 (Horner and Currie 1994) and falls between the late nestling-early juvenile range (Horner et al. 2000). Overall, the Sandstone Basin locality accounts for potentially four hadrosaurid individuals of varying ages ranging from early nestlings to early juveniles. Additionally, the articulated postcranial skeleton of a late nestling *Edmontosaurus* cf. *annectens* individual (Wosik et al. 2017) was also discovered here. This high density of rare hadrosaurid nestling bones suggests that Sandstone Basin may have been in close proximity to a nesting ground, but without evidence of eggshell material at this site, any conclusions about nesting horizons in the Hell Creek Formation remain purely speculative.

Ontogenetic Variability within the Cranium

Of the 37 total characters used in this analysis (Table 1), 14 were determined to be ontogenetically variable across the nestling-adult size range, with the majority belonging to the dentary. The dentary exhibits 10 ontogenetically variable characters from a total of 22 that were used in this analysis, with four containing the nestling dentary (UCMP 235860). The number of alveoli in the dentary is known to increase with ontogeny in hadrosaurids (Horner et al. 2004; Bramble et al. 2017) and is reflected here in *Edmontosaurus* (Character 1). Nestlings exhibit approximately 10 alveoli on each dentary, juveniles increase this count to about 35 alveoli, and subadults and adults tend to exceed 45 alveoli. This is noteworthy because much of the ontogenetic changes that occur in the dentary of *Edmontosaurus* may likely be associated with the addition of tooth families (columns of multi-generational teeth within each alveolus), increase in the amount of tooth generations, and the consequent anteroposterior extension and increased depth of the dental battery itself (LeBlanc et al. 2016, Bramble et al. 2017). The region anterior to the dental battery, which consists of the diastema, or edentulous margin, and the symphyseal process, subsequently undergoes corresponding allometric shifts towards a more anteroposterior expanded edentulous margin (Character 38) and a more acute angulation between the mandibular symphysis and the lateral margin of the dentary (Character 44). However, many of the characters referring to ratios or degrees of curvature (Characters 41–43, 46, 48) vary ontogenetically without a distinct directional pattern of change. In particular, the coronoid process inclines more anteriorly in adults than in subadults (Character 48), but

Table 1. Ontogenetic character state comparison of *Edmontosaurus annectens* using the character matrix from Xing et al. (2017). Dentary scores for the adult size class were used directly from Xing et al. (2017).

Bone Element	Character No.	Size Class				Ontogenetic variability
		Nestling	*Juvenile*	*Subadult*	*Adult*	
Dentary	1	0	1	2	2	Y
	38	1 (0.27)	2 (0.31-0.37)	3 (0.51)	3	Y
	39	1 (165)	1 (152-156)	1 (162)	1	N
	40	0 (132)	0 (131-139)	0 (145)	0	N
	41	0 (15)	1 (20-24)	0 (13)	0	Y
	42	-	0+1	1	0+1	Y
	43	-	0+1	1	0	Y
	44	-	0 (29-17)	1 (6)	1	Y
	45	-	0	0	0	N
	46	-	0+1	1	1	Y
	47	1	1	1	1	N
	48	1 (82)	1 (71-80)	1 (78)	2	Y
	49	-	1+2	2	2	Y
	50	-	1	1	1	N
	51	-	0+1	1	0	Y
	52	-	1	1	1	N
	53	1 (163)	1 (161)	1 (144)	1	N
	54	-	1	1	1	N
	55	1	1	1	1	N
	56	0?	2	2	2	Y?
	57	1	1	1	1	N
	58	1	1	1	1	N
Surangular	59	1	1	-	1	N
	60	1	1	-	1	N
	61	-	1	1	1	N
	62	2	2	2	2	N
	63	-	1	-	1	N
	64	-	1	0	1	Y
	65	-	1	1	1	N
	66	0 (162)	0+1 (148-158)	-	1 (145)	Y
Quadrate	129	0 (156)	0 (161-162)	1 (145)	0 (152-165)	Y
	130	1*	1	1	1	N
	131	1* (25)	1 (33-38)	1 (38)	1 (35-38)	N
	132	1	1	1	1	N
	133	-	0	0	0	N
	134	1* (0.95)	1 (0.86)	1 (0.87)	1 (0.86-0.95)	N
	135	1	1	1	1	N
	136	0	1	1	1	Y

juveniles exhibit a wide range of variation that spans from 71–80° from the horizontal axis of the dentary. Additionally, our ontogenetic comparison presents multiple conditions for the shape of the apex of the coronoid process (Characters 49, 51) particularly in juveniles suggesting that this region may have been more plastic.

Both the surangular and quadrate increase in robustness and are generally proportionately consistent through ontogeny. The degree of posterior curvature of the quadrate ramus in lateral view (Character 129) is often used to help distinguish hadrosaurines from lambeosaurines, but varies here from 145°–162° closely overlapping the prescribed threshold of 150° between the two character states. The lateral exposure of the quadratojugal notch of the quadrate (Character 136), sometimes referred to as the quadratojugal foramen, may also undergo a strong shift towards the closure, or absence, of this lateral exposure between the nestling and juvenile age range, although this is not certain given the disarticulated nature of the material. In hadrosaurid adults, the quadratojugal forms a lateral scarf joint with the dorsal half of the quadratojugal notch of the quadrate but meets against the anterior margin of the ventral half. This condition is already recognized in juveniles, which have substantial striations for soft tissue attachment within a large depression along the dorsal half of the quadratojugal notch that would host the lateral scarf joint connection with the quadratojugal. However, the nestling (UCMP 235859) provides no evidence for a lateral scarf joint connection anywhere along the quadratojugal notch of the quadrate. Instead, it appears that the entire posterior margin of the quadratojugal would meet with the anterior margin of the quadrate along the quadratojugal notch. Therefore, it is possible that the lateral exposure, or quadratojugal foramen, may be present in nestlings but closed by the juvenile stage in *Edmontosaurus*. This type of change is not uncommon when considering the malleable qualities of cranial sutures in the extant *Alligator mississippiensis* (Bailleul et al. 2016) and ontogenetic closure of cranial foramina in diplodocid dinosaurs (Woodruff et al. 2017) and cranial fenestra in pachycephalosaurs (Horner and Goodwin 2009).

Taxonomic Identification of Juveniles

The cranium of hadrosaurid dinosaurs undergoes significant morphological changes through ontogeny, which can hinder proper taxonomic identification of juvenile ontogimorphs (e.g., Dodson 1975, Evans et al. 2005, Evans 2010, Prieto-Márquez 2011, Campione and Evans 2011, McGarrity et al. 2013). Historically, hadrosaurine hadrosaurids closely related to *Edmontosaurus* consisted of five individually named taxa based on numerous complete specimens (Lull and Wright 1942, Campione and Evans 2011). However, rigorous morphometric analyses of the cranium using a comprehensive sample of complete edmontosaur skulls identified only two valid species, *E. annectens* and *E. regalis* (Campione and Evans 2011). The results strongly suggested that cranial variation previously used to diagnose certain edmontosaur species could be explained by ontogenetic size increases and allometric growth (Campione and Evans 2011). This is further reflected in *E. annectens* from our comparison of the presently described nestling material with other *E. annectens* specimens across an ontogenetic perspective, which reveals that many characters used in hadrosaur matrices (e.g., Prieto-Márquez 2010; Xing et al. 2017) exhibit varied degrees of ontogenetic variation.

This brings into question the taxonomic status of *Ugrunaaluk kuukpikensis*, a hadrosaurine hadrosaurid closely related to *Edmontosaurus* erected on the basis of disassociated juvenile cranial material from the Liscomb Bonebed in the Prince Creek Formation (lower Maastrichtian) of northern Alaska (Mori et al. 2016). The authors reported that *U. kuukpikensis*, which was previously referred to *Edmontosaurus* sp. (Gangloff and Fiorillo 2010, Campione and Evans 2011, Xing et al. 2014), possessed a collection of diagnostic cranial characteristics and argued that the juvenile stage of this taxon was diagnostically valid when compared with other Edmontosaurini taxa. Although we agree that *U. kuukpikensis* belongs in Edmontosaurini, the species-level analysis of Mori et al. (2016) is confounded by several variables, particularly lacking comparison with similarly-sized juvenile material of both *Edmontosaurus* species (Xing et al. 2014, 2017). Although associated juvenile individuals of *E. regalis* and *E. annectens* are either not preserved in the fossil record or very rare (Prieto-Márquez 2014, Wosik et al. 2017), respectively, there are many instances of monodominant bonebeds for both species (e.g., Christians 1992, Colson et al. 2004, Bell and Campione 2014, Evans et al. 2015, Wosik and Evans 2015, Ullmann et al. 2017) that provide excellent samples for studying ontogenetic changes in the cranium (Fig. 7).

Without evidence from ontogenetic studies that include similarly-sized juveniles of both taxa, neither *Edmontosaurus* species can be conclusively excluded as possible taxonomic identities of *U. kuukpikensis*. Three characteristics were used to distinguish *U. kuukpikensis* from *E. annectens*: a dorsoventrally short and elongate maxilla, a relatively gracile jugal, and a short symphyseal

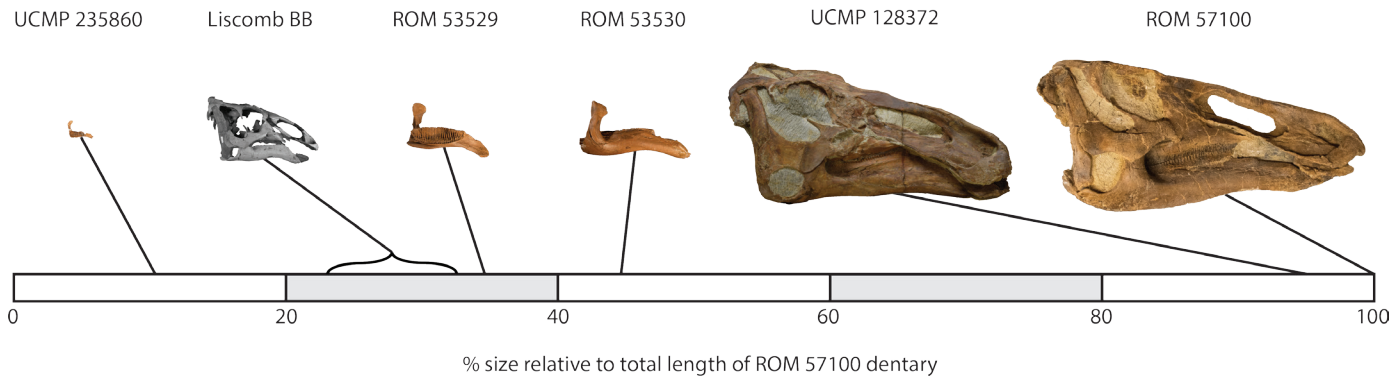

Figure 7. Growth series of *Edmontosaurus annectens* skulls and dentaries scaled to size (dentary length of ROM 57100 = 750 cm) highlighting the size difference between nestlings and adults. Liscomb Bonebed (BB) skull reconstruction modified from Mori et al. 2016.

process of the dentary. However, we demonstrate here that the dentary is significantly plastic through ontogeny and a ratio between the length of the symphyseal process and total dentary length reveals that *U. kuukpikensis* (UAMES 12941 [40%], UAMES 4946 [41%]) cannot be differentiated from slightly larger juvenile individuals of *E. annectens* (ROM 53529 [44%], ROM 53530 [42%]). When compared with *E. regalis*, regression analyses were based on small sample sizes of less than 10 individuals of *U. kuukpikensis* (Mori et al. 2016, fig. 7e) and do not overlap in size. Therefore, assumptions were made about the juvenile state in *E. regalis* of the vestibular promontory of the premaxilla and the width of the jugal process based on the presence or absence in juveniles of the sister taxon, *E. annectens*.

Based on the ontogenetic comparisons presented here, we agree with Xing et al. (2017) that *U. kuukpikensis* at current does not represent a valid taxon and should instead be regarded as *Edmontosaurus* sp. (Gangloff and Fiorillo 2010, Campione and Evans 2011, Xing et al. 2014) until additional, similarly-sized juvenile material attributable to both *E. annectens* and *E. regalis* and/or larger, preferably adult material of *U. kuukpikensis* becomes available. The Alaskan material should also be further investigated histologically to determine whether the hadrosaurid assemblage from the Prince Creek Formation does indeed belong to juveniles or whether this is a dwarf taxon (Sander et al. 2006) or dwarf morphotype, which may offer an important role in properly interpreting migration patterns and population structure among hadrosaurids (Fiorillo and Gangloff 2001, Chinsamy et al. 2012, Wosik et al. 2015).

CONCLUSION

The collection of hadrosaurine cranial material described herein denotes the first substantial evidence of nestling-sized cranial material from the intensely sampled end-Cretaceous Hell Creek Formation of the northwestern United States. Using an entire ontogenetic series of the dentary, surangular, and quadrate for the hadrosaurine *Edmontosaurus annectens*, we identified additional ontogenetically variable characters that are consistently used in assessing phylogenetic relationships among hadrosaurids. Although the quadrate and surangular generally develop isometrically, the dentary undergoes significant ontogenetic changes, particularly in relation to the expansion of the dental battery, and exhibits a high degree of intraspecific variability through ontogeny. As additional specimens are discovered and described, it is vital that they be included in a thorough ontogenetic assessment to recognize any further ontogenetically variable characters and morphologies. Meanwhile, taxonomic identification of new taxa should be strictly restricted to properly distinguishable adult individuals until enough research is available to develop juvenile-only matrices for a large range of complementing taxa or ontogenetic invariability within a taxon has been irrefutably established.

ACKNOWLEDGMENTS

Access to specimens was facilitated by K. Seymour (ROM) and P. Holroyd (UCMP). Additional preparation of the nestling specimens was done by S. Sugimoto (ROM). The cover illustration for this article was done by D. M. Yeider. Funding for this project was provided by a Doris O. and Samuel P. Welles Research Fund (to MW) from the UCMP and a Natural Sciences and Engineering Research Council of Canada Discovery Grant RGPIN 355845 (to DCE). Extensive feedback from D. McLennan and comments from D.M. Erwin, D. Fastovsky, and an anonymous reviewer greatly enhanced the manuscript. We thank

the Twitchell family for their long-term support of field work by the UCMP, W.A. Clemens, and crews on their ranch. W.A. Clemens provided access to his field notes and detailed accounts of UCMP fieldwork in the early 1980's when the specimens described in this study were collected under his leadership. D. Melton and G. Liggett of the Bureau of Land Management Office facilitated access to land under their management.

LITERATURE CITED

Bailleul, A.M, J.B. Scannella, J.R. Horner, and D.C. Evans. 2016. Fusion patterns in the skulls of modern archosaurs reveal that sutures are ambiguous maturity indicators for the Dinosauria. *PLoS ONE* 11(2):e0147687.

Bell, P.R., and N.E. Campione. 2014. Taphonomy of the Danek Bonebed: a monodominant *Edmontosaurus* (Hadrosauridae) bonebed from the Horseshoe Canyon Formation, Alberta. *Canadian Journal of Earth Sciences* 51:992–1006.

Bramble, K., A. R. H. LeBlanc, D. O. Lamoureux, M. Wosik, and P. J. Currie. 2017. Histological evidence for a dynamic dental battery in hadrosaurid dinosaurs. *Scientific Reports* 7:15787.

Brown, B. 1907. The Hell Creek beds of the Upper Cretaceous of Montana. *American Museum of Natural History Bulletin* 23:823–845.

Brown, B. 1912. A crested dinosaur from the Edmonton Cretaceous. *Bulletin of the American Museum of Natural History* 31:131–136.

Brown, B. 1916. A new crested trachodont dinosaur *Prosaurolophus maximus*. *Bulletin of the American Museum of Natural History* 35:701–708.

Brown, C.M., N.E. Campione, and D.C. Evans. 2013. Body size related taphonomic biases in the latest Maastrichtian; Implications for the end-Cretaceous extinction. *Journal of Vertebrate Paleontology* 33(Supplement):95.

Campione, N.E., and D.C. Evans. 2011. Cranial growth and variation in edmontosaurs (Dinosauria: Hadrosauridae): implications for latest Cretaceous megaherbivore diversity in North America. *PLoS ONE* 6(9):e25186.

Carpenter, K. 1982. Baby dinosaurs from the Late Cretaceous Lance and Hell Creek formations and a description of a new species of theropod. *Rocky Mountain Geology* 20(2):123–134.

Chinsamy, A., D.B. Thomas, A.R. Tumarkin-Deratzian, and A.R. Fiorillo. 2012. Hadrosaurs were perennial polar residents. *The Anatomical Record* 295(4):610–614.

Christians, J.P. 1992. Taphonomy and sedimentology of the Mason Dinosaur Quarry, Hell Creek Formation (Upper Cretaceous), South Dakota. M.S. thesis, University of Wisconsin, Madison, WI.

Clemens, W.A, and J.H. Hartman. 2014. From *Tyrannosaurus* rex to asteroid impact: Early studies (1901–1980) of the Hell Creek Formation in its type area. In G.P. Wilson, W.A. Clemens, J.R. Horner, and J.H. Hartman (eds.). Through the end of the Cretaceous in the type locality of the Hell Creek Formation in Montana and adjacent areas. *Geological Society of America Special Papers* 503:1–88.

Colson, M.C., R.O. Colson, and R. Nellermoe. 2004. Stratigraphy and depositional environments of the upper Fox Hills and lower Hell Creek Formations at the Concordia Hadrosaur Site in northwestern South Dakota. *Rocky Mountain Geology* 39(2):93–111.

Cope, E.D. 1869. Synopsis of the extinct Batrachia, Reptilia, and Aves of North America. *Transactions of the American Philosophical Society* 14:1–252.

Dodson, P. 1975. Taxonomic implication of relative growth in lambeosaurine hadrosaurs. *Systematic Zoology* 24(1):37–54.

Dollo, L. 1888. Iguanodontidae et Camptonotidae. *Comptes Rendus hebdomadaires de l'Academie des Sciences, Paris* 106:775–777.

Evans, D.C. 2010. Cranial anatomy and systematics of *Hypacrosaurus altispinus*, and a comparative analysis of skull growth in lambeosaurine hadrosaurids (Dinosauria: Ornithischia). *Zoological Journal of the Linnean Society* 159(2):398–434.

Evans, D.C., C.A. Forster, and R.R. Reisz. 2005. The type specimen of *Tetragonosaurus* erectofrons (Ornithischia: Hadrosauridae) and the identification of juvenile lambeosaurines. Pp. 349–366 *in* P.J. Currie and E.B. Koppelhus (eds.). Dinosaur Provincial Park: A spectacular ancient ecosystem revealed. Indiana University Press, Bloomington.

Evans, D.C., D.A. Eberth, and M.J. Ryan. 2015. Hadrosaurid (*Edmontosaurus*) bonebeds from the Horseshoe Canyon Formation (Horsethief Member) at Drumheller, Alberta, Canada: geology, preliminary taphonomy, and significance. *Canadian Journal of Earth Sciences* 52(8):642–654.

Fastovsky, D.E., and A. Bercovici. 2016. The Hell Creek Formation and its contribution to the Cretaceous-Paleogene extinction: A short primer. *Cretaceous Research* 57:368–390.

Fiorillo, A.R., and R.A. Gangloff. 2001. The caribou migration model for Arctic hadrosaurs (Dinosauria: Ornithischia): a reassessment. *Historical Biology* 15(4):323–334.

Gangloff, R.A., and A.R. Fiorillo. 2010. Taphonomy and paleoecology of a bonebed from the Prince Creek Formation, North Slope, Alaska. *PALAIOS* 25(5):299–217.

Garstka, W.R., and D.A. Burnham. 1997. Posture and stance of *Triceratops*: evidence of a digitigrade manus and cantilever vertebral column. Pp. 385–391 in D.L Wolberg, E. Stump, and G.D. Rosenberg (eds.). Dinofest International. Philadelphia Academy of Natural Science, Philadelphia.

Godefroit, P., S.L. Hai, T.X. Yu, and P. Lauters. 2008. New hadrosaurid dinosaurs from the uppermost Cretaceous of northeastern China. *Acta Palaeontologica Polonica* 53:47-74.

Goodwin, M.B., and J.R. Horner. 2014. Cranial morphology of a juvenile *Triceratops* skull from the Hell Creek Formation, McCone County, Montana, with comments on the fossil record of ontogenetically younger skulls. In G.P. Wilson, W.A. Clemens, J.R. Horner, and J.H. Hartman (eds.). Through the end of the Cretaceous in the type locality of the Hell Creek Formation in Montana and adjacent areas. *Geological Society of America Special Papers* 503:333–348.

Goodwin, M.B., W.A. Clemens, J.R. Horner, and K. Padian. 2006. The smallest known *Triceratops* skull: New observations on ceratopsid cranial anatomy and ontogeny. *Journal of Vertebrate Paleontology* 26(1):103–112.

Hall, J.P. 1993. A juvenile hadrosaurid from New Mexico. *Journal of Vertebrate Paleontology* 13(3):367–369.

Hartman, J.H. 2002. The Hell Creek Formation and the early picking of the Cretaceous-Tertiary boundary in the Williston Basin. In J.H. Hartman, K.R. Johnson, and D.J. Nichols (eds.). The Hell Creek Formation and the Cretaceous-Tertiary boundary in the Northern Great Plains: An integrated continental record of the end of the Cretaceous. *Geological Society of America Special*

Papers 361:1–8.
Horner, J.R., and P.J. Currie. 1994. Embryonic and neonatal morphology and ontogeny of a new species of *Hypacrosaurus* (Ornithischia, Lambeosauridae) from Montana and Alberta. Pp. 312–336 *in* K. Carpenter, K.F. Hirsch, and J.R. Horner (eds.). Dinosaur Eggs and Babies. Cambridge University Press, Cambridge.
Horner, J.R., and M.B. Goodwin. 2006. Major cranial changes during Triceratops ontogeny. *Proceedings of the Royal Society B* 273(1602):2757–2761.
Horner, J.R., and M.B. Goodwin. 2009. Extreme cranial ontogeny in the Upper Cretaceous dinosaur *Pachycephalosaurus*. *PLoS ONE* 4(10):e7626.
Horner, J.R., and R. Makela. 1979. Nest of juveniles provides evidence of family structure among dinosaurs. *Nature* 282:296–298.
Horner, J.R., A. de Ricqles, and K. Padian. 2000. Long bone histology of the hadrosaurid dinosaur *Maiasaura peeblesorum*: growth dynamics and physiology based on an ontogenetic series of skeletal elements. *Journal of Vertebrate Paleontology* 20(1):115–129.
Horner, J.R., K. Padian, and A. de Ricqles. 2001. Comparative osteohistology of some embryonic and perinatal archosaurs: developmental and behavioral implications for dinosaurs. *Paleobiology* 27(1):39-58.
Horner, J.R., D.B. Weishampel, and C.A. Forster. 2004. Hadrosauridae. Pp. 438–463 *in* D.B. Weishampel, P. Dodson, and H. Osmólska (eds.). The Dinosauria. University of California Press, Berkeley.
Horner, J.R., M.B. Goodwin, and N. Myhrvold. 2011. Dinosaur census reveals abundant *Tyrannosaurus* and rare ontogenetic stages in the Upper Cretaceous Hell Creek Formation (Maastrichtian), Montana, USA. *PLoS ONE* 6(2):e16574.
Hu, C.Z. 1973. A new hadrosaur from the Cretaceous of Zhucheng, Shantung. *Acta Geologica Sinica* 2:179–206.
Jackson, F.D., and D.J. Varricchio. 2016. Fossil egg and eggshells from the Upper Cretaceous Hell Creek Formation, Montana. *Journal of Vertebrate Paleontology* 36(5):e1185432.
Keenan, S.W., and J.B. Scannella. 2014. Paleobiological implications of a *Triceratops* bonebed from the Hell Creek Formation, Garfield County, northeastern Montana. In G.P. Wilson, W.A. Clemens, J.R. Horner, and J.H. Hartman (eds.). Through the end of the Cretaceous in the type locality of the Hell Creek Formation in Montana and adjacent areas. *Geological Society of America Special Papers* 503:349–364.
Kobayashi, Y, and Y. Azuma. 1999. Cranial material of a new iguanodontian dinosaur from the Lower Cretaceous Kitadani Formation of Japan. *Journal of Vertebrate Paleontology* 19(Supplement):57A.
Lambe, L.M. 1914. On *Gryposaurus notabilis*, a new genus and species of trachodont dinosaur from the Belly River Formation of Alberta, with a description on the skull of *Chasmosaurus belli*. *Ottawa Naturalist* 27:145–155.
Lambe, L.M. 1917. A new genus and species of crestless hadrosaur from the Edmonton Formation of Alberta. *The Ottawa Naturalist* 31(7):65–73.
LeBlanc, A.R.H., R.R. Reisz, D.C. Evans, and A.M. Bailleul. 2016. Ontogeny reveals function and evolution of the hadrosaurid dinosaur dental battery. *BMC Evolutionary Biology* 16:152.
Lull, R.S., and N.E. Wright. 1942. Hadrosaurian dinosaur of North America. *Geological Society of America Special Papers* 40:1–242.
Lyson, T.R., and N.R. Longrich. 2011. Spatial niche partitioning in dinosaurs from the latest Cretaceous (Maastrichtian) of North America. *Proceeding of the Royal Society B* 278:1158–1164.
Marsh, O.C. 1881. Principal characters of the American Jurassic dinosaurs, Part IV. *American Journal of Science* 21:417–423.
Marsh, O.C. 1892. Notice of new reptiles from the Laramie Formation. *American Journal of Science, Series 3* 43:449–453.
Mathews, J.C., S.L. Brusatte, S.A. Williams, and M.D. Henderson. 2009. The first *Triceratops* bonebed and its implications for gregarious behavior. *Journal of Vertebrate Paleontology* 29(1):286–290.
McGarrity, C.T., N.E. Campione, and D.C. Evans. 2013. Cranial anatomy and variation in *Prosaurolophus maximum* (Dinosauria: Hadrosauridae). *Zoological Journal of the Linnean Society* 167(4):531–568.
Mori, H., P.S. Druckenmiller, and G.M. Erickson. 2016. A new Arctic hadrosaurid from the Prince Creek Formation (lower Maastrichtian) of northern Alaska. *Acta Palaeontologica Polonica* 61(1):15–32.
Norman, D.B. 2002. On Asian ornithopods (Dinosauria: Ornithischia). 4. *Probactrosaurus* Rozhdestvensky, 1966. *Zoological Journal of the Linnean Society* 136:113–144.
Pearson, D.A., T. Schaefer, K.R. Johnson, D.J. Nichols, and J.P. Hunter. 2002. Vertebrate biostratigraphy of the Hell Creek Formation in southwestern North Dakota and northwestern South Dakota. In J.H. Hartman, K.R. Johnson, and D.J. Nichols (eds.). The Hell Creek Formation and the Cretaceous-Tertiary boundary in the Northern Great Plains: An integrated continental record of the end of the Cretaceous. *Geological Society of America Special Papers* 361:145–168
Prieto-Márquez, A. 2010. Global phylogeny of Hadrosauridae (Dinosauria: Ornithopoda) using parsimony and Bayesian methods. *Zoological Journal of the Linnean Society* 159(2):435–502.
Prieto-Márquez, A. 2011. Cranial and appendicular ontogeny of *Bactrosaurus johnsoni*, a hadrosauroid dinosaur from the Late Cretaceous of northern China. *Palaeontology* 54(4):773–792.
Prieto-Márquez, A. 2014. A juvenile *Edmontosaurus* from the late Maastrichtian (Cretaceous) of North America: implications for ontogeny and phylogenetic inference in saurolophine dinosaurs. *Cretaceous Research* 50:282–303.
Prieto-Márquez, A., and M.F. Guenther. 2018. Perinatal specimens of *Maiasaura* from the Upper Cretaceous of Montana (USA): insights into the early ontogeny of saurolophine hadrosaurid dinosaurs. *PeerJ* 6:e4734.
Prieto-Márquez, A., and J.R. Wagner. 2009. *Pararhabdodon isonensis* and *Tsintaosurus spinorhinus*: a new clade of lambeosaurine hadrosaurids from Eurasia. *Cretaceous Research* 30:1238–1246.
Russell, D.A, and M. Manabe. 2002. Synopsis of the Hell Creek (uppermost Cretaceous) dinosaur assemblage. In J.H. Hartman, K.R. Johnson, and D.J. Nichols (eds.). The Hell Creek Formation and the Cretaceous-Tertiary boundary in the Northern Great Plains: An integrated continental record of the end of the Cretaceous. *Geological Society of America Special Papers* 361:169–176
Sander, P.M., O. Mateus, T. Laven, and N. Knötschke. 2006. Bone histology indicates insular dwarfism in a new Late Jurassic sauropod dinosaur. *Nature* 441:739–741.
Scannella, J.B., and D.W. Fowler. 2014. A stratigraphic survey of *Triceratops* localities in the Hell Creek Formation, northeastern

Montana (2006–2010). In G.P. Wilson, W.A. Clemens, J.R. Horner, and J.H. Hartman (eds.). Through the end of the Cretaceous in the type locality of the Hell Creek Formation in Montana and adjacent areas. *Geological Society of America Special Papers* 503:313–332

Seeley, H.G. 1887. On the classification of the fossil animals commonly named Dinosauria. *Proceedings of the Royal Society of London* 43:165–171.

Sprain, C.J., P.R. Renne, G.P. Wilson, and W.A. Clemens. 2015. High-resolution chronostratigraphy of the terrestrial Cretaceous-Paleogene transition and recovery interval in the Hell Creek region, Montana. *Geological Society of America Bulletin* 127:393–409.

Tanke, D.H., and M.K. Brett-Surman. 2001. Evidence of hatchling- and nestling-sized (Reptilia: Ornithischia) from Dinosaur Provincial Park (Dinosaur Park Formation: Campanian), Alberta. Pp. 206–218 *in* D.H. Tanke and K. Carpenter (eds.). Mesozoic Vertebrate Life. Indiana University Press, Bloomington.

Tokaryk, T.T. 1997. First evidence of juvenile ceratopsians (Reptilia: Ornithischia) from the Frenchman Formation (late Maastrichtian) of Saskatchewan. *Canadian Journal of Earth Sciences* 34(10):1401–1404.

Ullmann, P.V., A. Shaw, R. Nellermoe, and K.J. Lacovara. 2017. Taphonomy of the Standing Rock Hadrosaur Site, Corson County, South Dakota. *PALAIOS* 32(12):779–796.

Wang, R.F, H.L. You, S.Z. Wang, S.C. Xu, J. Yi, L.J. Xie, L. Jia, and H. Xing. 2017. A second hadrosauroid dinosaur from the early Late Cretaceous of Zuoyun, Shanxi Province, China. *Historical Biology* 29(1):17–24.

Wagner, J.R. 2001. The hadrosaurian dinosaurs (Ornithischia: Hadrosauria) of Big Bend National Park, Brewster County, Texas, with implications for Late Cretaceous Paleozoogeography. Unpubished Master's Thesis. Austin: Texas Tech University. pp. 1–417.

Weishampel, D.B., and J.R. Horner. 1986. The hadrosaurid dinosaurs of the Iren Dabasu Formation (People's Republic of China, Late Cretaceous). *Journal of Vertebrate Paleontology* 6:38–45.

Weishampel, D.B., D.B. Norman, and D. Grigorescu. 1993. *Telmatosaurus transslyvanicus* from the Late Cretaceous of Romania: the most basal hadrosaurid dinosaur. *Paleontology* 36(2):261–285.

Woodruff, D.C., D.W. Fowler, and J.R. Horner. 2017. A new multifaceted framework for deciphering diplodocid ontogeny. *Palaeontologia Electronica* 20.3.43A:1–53.

Wosik, M., and D.C. Evans. 2015. Ontogenetic long bone histology of *Edmontosaurus annectens* (Ornithischia: Hadrosauridae) from a monodominant bonebed. *Journal of Vertebrate Paleontology* 35(Supplement):241.

Wosik, M., M.B. Goodwin, and D.C. Evans. 2017. A nestling-sized skeleton of *Edmontosaurus* (Ornithischia, Hadrosauridae) from the Hell Creek Formation of northeastern Montana, USA, with an analysis of ontogenetic limb allometry. *Journal of Vertebrate Paleontology* 37(6):e1398168.

Xing, H., J.C. Mallon, and M.L. Currie. 2017. Supplementary cranial description of the types of *Edmontosaurus regalis* (Ornithischia: Hadrosauridae), with comments on the phylogenetics and biogeography of Hadrosaurinae. *PLoS ONE* 12(4):e0175253.

Xing, H., A. Prieto-Márquez, W. Gu, and T.X. Yu. 2012. Re-evaluation and phylogenetic analysis of *Wulagasaurus dongi*, a hadrosaurine dinosaur from the Maastrichtian of northeast China. *Vertebrata PalAsiatica* 50(2):160–169.

Xing, H., X. Zhao, K. Wang, D. Li, S. Chen, J.C. Mallon, Y. Zhang, and X. Xu. 2014. Comparative osteology and phylogenetic relationships of *Edmontosaurus* and *Shantungosaurus* (Dinosauria: Hadrosauridae) from the Upper Cretaceous of North America and East Asia. *Acta Geologica Sinica* 88(6):1623–1652.

Xing, H., D.Y. Wang, F.L. Han, C. Sullivan, Q.Y. Ma, Y.M. He, D.W.E. Hone, R. Yan, F. Du, and X. Xu. 2014. A new basal hadrosauroid dinosaur (Dinosauria: Ornithopoda) with transitional features from the Late Cretaceous of Henan Province, China. *PLoS ONE* 9(6):e98821.

Appendix 1. Character descriptions corresponding to those of Xing et al. (2017). Characters preceded with an (*) were scored for the nestling material described in this paper. Characters highlighted in bold displayed various degrees of ontogenetic variability. Characters corresponding to Prieto-Márquez and Wagner (2009) are designated as =P-M&W character number. Character scores are listed in Table 1.

1. ***Maximum number of dental alveoli (tooth positions) in the dentary dental battery (modified from Horner et al. 2004 character 1): (0) 30 or fewer; (1) 31 to 45; (2) more than 45.**

Dentary

38. ***Ratio between the length of the edentulous slope anterior to the dentary dental battery (not including the anterior most portion which contacts the predentary) and the horizontal distance between the first tooth position and the posterior end of the coronoid process (=P-M&W character 37): (0) less than 0.20; (1) 0.20 to 0.31; (2) greater than 0.31 and up to 0.45; (3) greater than 0.45.**
39. *Angle between the edentulous slope of the dentary anterior portion and the level (=P-M&W character 38): (0) less than 150º; (1) 150º or greater.
40. *Angle between the slope of the dentary anterior region that contacts the predentary and the horizontal (modified from P-M&W character 39): (0) greater than 130º; (1) 115º to 130º; (2) less than 115º.
41. ***Degree of the downward deflection of the anterior part of the dentary that contacts the predentary, measured as the angle between the ventral margin of the anterior part of the dentary ramus and the dorsolateral margin of the posterior part of the ramus (modified from P-M&W character 40): (0) faintly deflected ventrally, with the angle less than 17º; (1) moderately deflected ventrally, with the angle between 17º to 25º; (2) markedly deflected ventrally, with the angle greater than 25º.**
42. **Ratio between the horizontal distance from the posterior margin of the coronoid process to the posteriormost end of the deflected ventral margin of the dentary and horizontal distance from the posterior margin of the coronoid process to the first alveolus (=P-M&W character 41): (0) greater than 0.78; (1) 0.66 to 0.78; (2) less than 0.66.**
43. **Ratio between the maximum mediolateral width of the dentary symphyseal region and the minimum breadth of the dentary posterior to the dentary symphyseal region in dorsal view (modified from P-M&W character 42): (0) up to 1.65; (1) greater than 1.65 and up to 2.60; (2) more than 2.60.**
44. **Angle between the medial surface of dentary symphysis and the lateral surface of the anterior region of the dentary in ventral view (modified from P-M&W character 43): (0) greater than 15º; (1) up to 15º.**
45. General profile of the dorsal margin of the dentary anterior region that contacts the predentary in medial or lateral view (=P-M&W character 45): (0) a smooth, gradually descending dorsal margin in the anterodorsal region of the dentary; (1) a relatively steep dorsal margin, forming a prominent depression in the dentary symphyseal region.
46. **Degree of the lingual curvature of the dentary symphyseal region in anterior view (=P-M&W character 44): (0) markedly curved lingually, forming a nearly 90º lateroventral profile in anterior view; (1) gently curved lingually, forming a sloping, wide arcuate lateroventral profile in anterior view.**
47. *General profile of the dentary ventral margin below the coronoid process in lateral view (modified from P-M&W character 46): (0) a slightly bowed ventral margin below the coronoid process; (1) a well-developed bowed ventral margin below the coronoid process.
48. ***Coronoid process (modified from Godefroit et al. (2008) character 39): (0) vertical to the dorsal margin of the dentary or inclined posteriorly; (1) slightly inclined anteriorly, with an angle between 70º and 85º; (2) obviously inclined anteriorly, with an angle less than 70º.**
49. **Shape of the apex of the coronoid process in adults (modified from Horner et al. (2004) character 17): (0) only slightly expanded anteriorly, with less developed anterior and posterior margins; (1) markedly expanded anteroposteriorly, with well-developed anterior and posterior margins; (2) markedly expanded anteroposteriorly, with well-developed anterior and posterior margins, bearing a more pronounced posterior margin.**
50. Medial wall of the triangular depression on the posterior side of the coronoid process in posterior view (corresponding with Xing et al. (2014) character 50): (0) not extending to the base of the dorsal apex, whose width is about one-quarter of the maximum mediolateral width of the apex; (1) extending to the base of the dorsal apex, whose width is about one-third of the maximum mediolateral width of the apex.
51. **A sharp projection on the posterodorsal surface of the coronoid process of the dentary (=P-M&W character 49): (0) absent; (1) present.**
52. Development of the ridge on the medial side of the coronoid process of the dentary (=P-M&W character 50): (0) presence of a faint, projecting medially ridge on the medial surface of the coronoid process; (1) presence of a well-developed and expanded posteriorly ridge, forming the mediodorsal boundary of a depressed facet which contacts the anterodorsal process of the surangular.
53. *Angle between the lateral surface of the dentary portion anterior to the coronoid process and that of the dentary portion anteroventral to the coronoid process in dorsal or ventral view (=P-M&W character 51): (0) the lateral surface of the dentary portion ventral to the coronoid process is only slightly expanded laterally, with an angle greater than 165º; (1) the lateral surface of the dentary portion ventral to the coronoid process is remarkably expanded laterally, with an angle up to 165º.
54. Orientation of the longitudinal axis of the dentary occlusal surface relative to the lateral margin of the dentary in dorsal view (=P-M&W character 52): (0) presence of a relatively inclined longitudinal axis, forming an angle of about 20º with the lateral margin of the dentary; (1) presence of a longitudinal axis running parallel with the lateral margin of the dentary.
55. Lingual curvature of the longitudinal axis of the dentary occlusal surface in dorsal view (=P-M&W character 53): (0) present; (1) absent.
56. ***Position of the coronoid process relative to the**

Appendix 1 (cont.). Character descriptions corresponding to those of Xing et al. (2017). Characters preceded with an (*) were scored for the nestling material described in this paper. Characters highlighted in bold displayed various degrees of ontogenetic variability. Characters corresponding to Prieto-Márquez and Wagner (2009) are designated as =P-M&W character number. Character scores are listed in Table 1.

dentary dental battery (modified from Horner et al. (2004) character 10): (0) the posterior margin of the coronoid process is located posterior to the posterior end of the dental battery; (1) the posterior margin of the coronoid process is overlapped with the posterior end of the dental battery; (2) the posterior margin of the coronoid process is located anterior to the posterior end of the dental battery.

57. *Degree of separation between the dentary dental battery and the coronoid process (=P-M&W character 55): (0) the coronoid process is not obviously separate from the dentary dental battery; (1) the coronoid process is obviously separate from the dentary dental battery, with the presence of a depressed buccal shelf separating the base of coronoid process from the dental battery.
58. *Anterodorsal inclination of the long axis of the dentary tooth row relative to the ventral margin of the middle part of the dentary ramus (corresponding with Wang et al. (2017) character 58): (0) present; (1) absent, the long axis of the tooth row is either generally parallel with the ventral margin of the middle region of the dentary ramus or slightly anteroventrally inclined relative to this margin.

Surangular

59. *Surangular foramen (corresponding with Norman 2002 character 27): (0) present; (1) absent.
60. *Surangular accessory foramen on the anterolateral surface of the surangular (corresponding with Kobayashi and Azuma (1999) character 15): (0) present; (1) absent.
61. Contact surface of the surangular anterodorsal process for the coronoid process of the dentary (modified from Xing et al. (2012) character 60): (0) the anterior half of the anterolateral surface of the anterodorsal process; (1) most of the anterolateral surface of the anterodorsal process.
62. *Participation of the surangular in the ventral side of the mandibular posterior part (modified from P-M&W character 59): (0) absent, surangular only participating in the lateral side of the mandibular posterior part; (1) present, surangular facing more laterally than ventrally; (2) present, surangular facing more ventrally than laterally.
63. **Strong upward curvature of the retroarticular process of the surangular (=P-M&W character 60): (0) absent; (1) present.**
64. Lateral profile of the surangular posteroventral corner ventral to the retroarticular process (corresponding with Xing et al. (2014) character 65): (0) broadly arcuate; (1) a nearly 90º angle.
65. General shape of the retroarticular process of the surangular (corresponding with Xing et al. (2014) character 66): (0) relatively robust in lateral view, forming a round, blunt posterodorsal extremity; (1) subtriangular in lateral view, forming a posterodorsally tapering extremity.
66. *Angle between the ventromedial margin of the anterior part of the surangular and that of the retroarticular process (modified from P-M&W character 61): (0) 150º or greater; (1) less than 150º.

Quadrate

129. ***Degree of the curvature of the quadrate in lateral view (angle between the long axis of the dorsal portion of the quadrate and the one of the ventral portion of the quadrate) (modified from Wagner (2001) character 35): (0) slightly curved posteriorly, with an angle more than 150º; (1) strongly curved posteriorly, with an angle up to 150º.**
130. *Position of the quadratojugal notch relative to the dorsoventral height of the quadrate (=P-M&W character 125): (0) the midpoint of the quadratojugal notch is located near half the dorsoventral height of the quadrate; (1) the midpoint of the quadratojugal notch is located well below half the dorsoventral height of the quadrate.
131. *Angle between the dorsal margin of the quadratojugal notch and the long axis of the quadrate (modified from P-M&W character 126): (0) greater than 40º; (1) up to 40º.
132. *General shape of the quadratojugal notch of the quadrate (modified from Weishampel and Horner (1986)): (0) semicircular and relatively deep anteroposteriorly, with the ventral margin of the notch which is slightly recurved and directed anteriorly; (1) wide arcuate and relatively shallow anteroposteriorly, with the ventral margin of the notch which is smooth and directed anteroventrally; (2) wide arcuate and relatively shallow anteroposteriorly, with the ventral margin of the notch which is slightly recurved and directed anteriorly.
133. Squamosal buttress (posterodorsal protuberance) on the posterior side of the dorsal end of the quadrate (modified from Weishampel and Horner (1986)): (0) presence of a well- developed protuberant buttress; (1) absence of the buttress or presence of a less developed faint buttress.
134. *Ratio between the anteroposterior length of the lateral condyle and the mediolateral width of the ventral end of the quadrate (modified from Weishampel et al. (1993) character 22): (0) up to 0.75; (1) more than 0.75.
135. *Elevation of the medial condyle of the quadrate in anterior view (modified from P-M&W character 129): (0) the medial condyle is slightly elevated upwards relative to the lateral condyle; (1) the medial condyle is remarkably elevated upwards relative to the lateral condyle.
136. ***Lateral exposure of the quadratojugal notch of the quadrate (modified from P-M&W character 198): (0) present; (1) absent.**